IFUSP/P 429

UNIVERSIDADE DE SÃO PAULO

INSTITUTO DE FÍSICA
CAIXA POSTAL 20516
01498 - SÃO PAULO - SP
BRASIL

publicações

IFUSP/P-429

OPTICAL ABSORPTION AND ELECTRON SPIN RESONANCE IN NATURAL, IRRADIATED AND HEATED SPODUMENE

by

Amando Siuiti Ito and Sadao Isotani
Instituto de Física, Universidade de São Paulo

Setembro/1983

OPTICAL ABSORPTION AND ELECTRON SPIN RESONANCE IN NATURAL, IRRADIATED AND HEATED SPODUMENE

Amando Siuiti Ito and Sadao Isotani

Instituto de Física da Universidade de São Paulo
C.P. 20516, São Paulo, SP, Brazil

ABSTRACT

Heat treatment and X and γ-Rays irradiation of lylac and colorless natural spodumene, $LiA\ell Si_2O_6$, have been studied. Irradiation produces a color change, from lylac or colorless to green. Irradiated samples heated at 200°C turn lylac and bleach at 400°C. Optical absorption spectra were decomposed into gaussian line shape bands and we observed that green and lylac centers are simultaneously created by irradiation. These centers are independent from each other. Optical absorption, EPR and X-Ray fluorescence results show the spectra of impurities, responsible by the presence of the created centers and indicated Mn participation in the process of centers creation and destruction. Decay kinetics of green and lylac centers have been studied and we observed that simple kinetic models do not apply to these cases. An empirical fit allowed the calculation of activation energies of the lylac and green centers decays. Discussions about the present results led us to propose a new model where the green and lylac centers are due to Mn^{3+} ions in two different $A\ell^{3+}$ sites, whose absorption are intensified by the interaction with an electron trapped in a neighbour oxygen.

1. INTRODUCTION

Spodumene is a single chain inosilicate made up of parallel chains of SiO_3 extended along the c axis (Deer et al, 1966). The chains are linked by ionic bonds through Li and $A\ell$ cations and the chemical formula of spodumene is $LiA\ell Si_2O_6$. Spodumene crystallizes in the monoclinic system and the unit cell contains four chemical formula units. There are four crystallographic equivalent sites for $A\ell^{3+}$ (M_1 sites) in the unit cell and the ions are octahedrally coordinated to oxygens. The Li ions are in larger and more distorted octahedral M_2 sites and there are also four M_2 sites in the unit cell. Impurities like Mn, Fe and Cr may substitute $A\ell$ ions at the M_1 sites and Na is usually found in the M_2 site. Different colors of spodumene are associated to the impurity ions present in the crystal structure. It is thought that yellow spodumene crystals have high iron content, the hiddenite variety have the green color due to chromium and the kunzite variety is lylac due to manganese (Schmitz and Lehmann, 1976; Hassan and Labib, 1978).

Qualitative descriptions of color changes in spodumene, either by irradiation as by heating were reported elsewhere (Hassan and Labib, 1978). Claffy (Claffy, 1953) proposed a classification of spodumene in two classes: chromian and non-chromian. The non-chromian samples showed luminescence and tenebrescence independent of color with UV or electron bean excitation, change of color with X-Ray or γ-Ray irradiation and annealing upon heating. The chromian samples did not show luminescence neither color changes by irradiation. The lylac kunzite color would be related to the presence of Mn and the high ratio Mn/Fe. The scheme shown in figure 1 indicates the transformation of color in non-chromian spodumene as proposed by Claffy.

Insert Figure 1

An association between valence and coordination state of Mn in kunzite and their color changes has been proposed by Schmitz and Lehmann (1976). They assumed that Mn^{2+} could be incorporated in the spodumene structure at the Si^{4+} distorted tetrahedral sites and suggested that the "lylac" optical absorption band (at 18,800 cm^{-1}) appears in irradiated colorless samples due to a change of Mn^{2+} to Mn^{3+} in Si^{4+} sites. Subsequent irradiation of lylac kunzite would transform Mn^{3+} to Mn^{4+} with the change of the "lylac" band in the "green" band (at 16,000 cm^{-1}). Hassan and Labib (1978) extended this model assigning the bands at 11,000 and 28,000 cm^{-1} to Fe^{2+} ions in $A\ell^{3+}$ and Si^{4+} sites, respectively.

In this report we present experimental observations about the optical absorption (OA) bands formation by irradiation in kunzite and their isothermal decay. These observations do not agree with the previous models and we propose a new model which accounts for the previous and present data.

2. EXPERIMENTAL

OA and EPR studies of colorless and lylac kunzite samples from Minas Gerais, Brazil, is the subject of the present work. Slices of 0.5 to 0.8 mm thickness and waffers of 4 to 10 mm thickness were cut with a Buehler diamond blade in a Buehler Isomet and polished with chromium oxide, alumina and diamond paste in a

Buehler Minimet. The samples were cut perpendicular to the c axis and to the cleavage planes (110).

The optical absorption spectra were obtained in a Carl Zeiss DMR 21 spectrophotometer, ranging from 4,000 to 50,000 cm^{-1}. Electron Paramagnetic Resonance (EPR) spectra were obtained in a JEOL JES-PE spectrometer operating at X-band. All spectra were obtained at room temperature.

X-Ray fluorescence analysis were done in a Rigaku Denki Co. X-Ray spectrometer. Irradiations of the samples were done with: a) X-Rays (K_αCu line) and a Victoreen ionization chamber monitored the exposition; b) γ-Rays from ^{60}Co with dosimetric measurements through the methods "cericerous", AECL red acrylic and UKAEA red perspex, in the plant of EMBRARAD S/A.

Heat treatments were done in air with a Forlabo furnace. Thermal stability was improved by reducing the volume of the furnace with the introduction of refractaries and metal plates. The samples were put in preheated furnaces at the desired annealing temperature. Finished the annealing time, the samples were quenched between two metal plates. The temperatures in the samples were measured with chromel-alumel thermocouples.

4. OPTICAL ABSORPTION MEASUREMENTS

We studied two groups of non-chromian samples: lylac with Mn/Fe >1 and colorless with Mn/Fe <1. Although they showed different colors and Mn/Fe relations, all samples showed morphological (growth axis, cleavage) and physical (density, refraction index) properties characteristic of spodumene.

The colors in spodumene have been assigned to the presence of Mn, Cr and Fe ions. So, we made X-Ray fluorescence analysis to see a possible correlation between color and impurity concentrations. The results are shown in Table I. All samples belong to non-chromian group and the color is correlated to the relation between the concentrations of Mn and Fe .

Insert Table 1

Optical Absorption:- The OA spectra of the three types of lylac spodumene are similar, and showed differences only in the intensity of the absorption bands. The samples with higher Mn concentrations showed higher bands. A characteristic spectrum of a lylac sample is shown in figure 2-a.

Insert Figure 2

In this figure the spectrum b is characteristic of colorless spodumene samples. Both lylac and colorless samples turn green by irradiation with X-Rays and γ-Rays, showing the same type of spectra of the type shown in figure 2-c.

Irradiation:- Spectra of lylac and colorless samples with successive higher doses with γ-Rays are shown in figures 3 and 4.

Insert Figures 3 and 4

Two important qualitative features are shown in these figures:

a) The colorless samples irradiated with low doses as 0.1 KGy showed the induction of green bands at about 16,000 cm^{-1}, which increases by turn with increasing irradiation dose. So, this experiment showed that the colorless-lylac transformation proposed by Claffy and incorporated in the Schmitz and Lehmann's model does not occur.

b) In colorless samples, the increasing of the green band is followed by an increase of the base line and by the simultaneous formation of the lylac band at about 19,000 cm^{-1} . This band is masked by the green band and is revealed by heating at 200°C.

Heating:- Heating the green samples obtained by irradiation to temperatures between 120° and 200° turns them lylac. At temperatures between 300° and 400°C the lylac band decayed and the samples turned colorless. Re-irradiation of the samples produced again the green and lylac bands, which by turn were bleached on heating.

The kinetics of the decay of the green and lylac bands were determined through the evolution of the OA spectra as function of the annealing times at the same temperature. In figure 5 we show the spectra of a sample annealed at 197°C. The green band shows a great decrease with 120 minutes of treatment, while the lylac band remains almost constant. Here, also, it was not observed the interconversion between the green and lylac bands.

Insert Figure 5

In Figure 6 we show by turn the effect of annealing at 372°C , where the lylac band practically disappears after 180 minutes of treatment.

Insert Figure 6

4. SPECTRA ANALYSIS

The OA spectra of spodumene can be a result of the superposition of different bands. Here we analysed the band shape of the observed bands, by assuming a superposition of gaussian bands. This line shape is found in the OA of impurities in solids with some deviation at the extrem of the bands (Dexter, 1954).

In a preliminary study of the line shape, we analysed the spectra of the lylac sample, by assuming that the lylac band is at 18,600 cm^{-1}. We adjusted the experimental points between 17,000 cm^{-1} and 20,000 cm^{-1} to a line shape of the form:

$$y = y_o \exp\left[-a(\nu-\nu_o)^b\right]$$

where y is the absorption coefficient, ν is the wave number, y_o , a , ν_o and b are constants. The value 2 obtained for b showed that this line shape is gaussian. In figure 7 we show the correlation between $(\ell n(y_o/y))^{1/2}$ as a function of the wave number ν . We see that a gaussian line at ν_o = 18,600 cm^{-1} fits quite well the lylac band.

Insert Figure 7

The OA spectra spodumene for both green and lylac samples were fit by a sum of gaussian lines:

$$y = \sum_i y_{oi} \exp|-(\nu-\nu_{oi})^2/2\sigma_i^2| + a + b\nu \quad .$$

The values of y_{oi} give the absorption coefficients of the i-th line, σ_i is the line width and ν_{oi} localizes the i-th line in the spectra. The parameters a and b are the usual base line parameters. A Least Square Gaussian Linearization Method (Bevington, 1969) was applied in order to fit the parameters of the above function to the experimental data. According to the initial values of parameters, different sets of parameters were obtained. In table 2 we show the mean values of parameteres obtained from different fits for sample 3. In figure 8, we show that the spectra of green irradiated spodumene is composed by two bands at 15,770 and 18,570 cm^{-1}.

Insert Table 2

Insert Figure 8

The analysis of the spectra of the samples irradiated with successive higher doses show the raising of the bands at 15,770 and 29,400 cm^{-1} and the saturation at 15 KGy (see Figure 9). This saturation shows that these bands are due to the filling of precursor centers by electrons or holes produced by irradiation and that the number of these precursor centers are not changed by irradiation. The saturation intensities increase with increasing concentration of Mn .

Insert Figure 9

5. THERMAL KINETICS

We carried out a systematic study of the thermal

decay kinetics of the 15,770 and 18,570 cm^{-1} bands by measuring the isothermal annealing of these bands at several temperatures. In figure 10 we show the behavior of the kinetics of the band at 15,770 cm^{-1} and figure 11 refers to the kinetics of the band at 18,570 cm^{-1}.

Insert Figure 10

Insert Figure 11

A first approach to fit the experimental data is the well known electron-hole pair recombination model of Randall-Wilkins (1940). Here the decay rate of the number of centers is proportional to the number of centers giving

$$y = y_o e^{-\beta t} ,$$

where y and y_o are the absorption coefficients at t and t_o, respectively, and $\beta=\beta_o \exp(-\Delta E/kT)$ is the decay rate with β_o being the frequency factor, ΔE the activation energy and T the absolute temperature. The $\ell n(y/y_o)$ versus t correlation showed that this model does not correspond to the observations in spodumene.

The next test of experimental data fit was with a bilinear model (Fuller and Moran, 1976) in which the recombination of the centers can occur randomly with two competitive centers. In this case:

$$\frac{dn}{dt} = -\beta n^2$$

and the solution of this equation gives for the absorption coefficient:

$$y = 1/(a+bt) \quad ,$$

where a and b are constants. The function, also, does not fit the experimental data.

Also, we applied a model of simultaneous recombination and retrapping, in which (Lushchick, 1956; Maxia et al, 1971):

$$\frac{dn}{dt} = -\beta \frac{B\ mn}{A(M-m) + Bn} \quad ,$$

where n is the trapped electron concentration, m the trapped hole concentration, M the concentration of electron traps, A the factor which gives the probability of retrapping and B the factor of recombination. We solved the above equation for m=n, and developed an algoritm for the calculation of the parameters, but it was not possible to fit the experimental data.

As simple models of kinetics were not able to fit our data, we applied a kinetic model of generical order m (Takeuchi et al, 1975). For the absorption coefficient:

$$\frac{dy}{dt} = -\beta y^m \quad ,$$

which gives:

$$(y/y_o)^{-m+1} = 1 + (m-1)y_o^{m-1}\beta t \quad .$$

The fit of the experimental data was done with a four points recurrence method (Isotani et al, 1982). The fit gives m values varying with the annealing temperature, showing that this model do not apply to the present data.

Finally, we consider here a model in which the kinetics is a sum of several processes of decay (Levy et al,1974). The thermal kinetics decay of the green and lylac bands are fit by:

$$y = \sum_{i=1}^{3} a_i \exp|-b_i t| \quad ,$$

where a_i and b_i are constants. This function gives a good fit as shown by the full lines in the figures 10 and 11. In table 3 we show the values of a_i and b_i .

Insert Table 3

The values of b_i show a slow process with $b \sim 10^{-3}$ minutes dominant for longer annealing times, an intermediate process with $b \sim 10^{-2}$ minutes dominant for annealing times between 10 to 50 minutes and a fast process with $b \sim 10^{-1}$ minutes dominant in the initial instants of annealing.

Two simple models can be assigned to the three exponential fit: a) three independent electron traps with different activation energies; b) a coupled recombination process similar to that proposed by Fuller and Moran (1976). Both models cannot be applied because of the large variations of a_i with the annealing temperatures.

In this way the present results show that the thermal kinetics decay in the green and lylac bands is very complex. The description of the population of free electrons and holes and trapped electrons and holes would be done through a model considering appropriate types of traps and recombination centers and the mobilities of electrons and holes. The solution of the resultant equations is very complex and beyond the scope of the present work.

6. ELECTRON PARAMAGNETIC RESONANCE MEASUREMENTS

We obtained the EPR spectra of crystals and powder samples of lylac and colorless spodumene. The spectra of spodumene obtained previously in the y and z magnetic axis show a complex pattern due to five types of octahedral and one tetrahedral Mn^{2+} line (Holuj, 1968). These lines are simplified by heating. The lines assigned to four complexes of octaedral Mn^{2+} are decreased by heating with the simultaneous raising of the fifth complex of octaedral Mn^{2+} (I) lines.

In figure 12 we show the EPR spectra of H//z spodumene.

Insert Figure 12

The spectrum of the figure 12-a show the Mn^{2+} (I) lines in natural spodumene. This spectrum is converted into figures 12-b by heating at 400°C. Re-irradiation does not change the Mn^{2+} (I) spectrum. The present observation shows that the heat transformation of octahedral Mn^{2+} is not reversible and is not directly associated with the formation of green and lylac bands. Also, tetrahedral Mn^{2+} lines were not observed in the spectra of the present natural, annealed and irradiated samples.

In figure 13 we show the powder EPR spectra of

lylac and colorless spodumene. The ratio between the lines of Fe^{3+} and Mn^{2+} is different as expected from different concentrations shown in table I. It was observed the exchange broadening of the lines in colorless samples, due to higher concentrations of Fe^{3+} which has a large exchange parameter J (Anderson and Weiss, 1953). After irradiation with γ-Rays it was not observed change in the powder spectra, although the color changed to green. Also, no change was observed for samples annealed at temperatures below 400°C. For higher temperatures, it was observed the disappearing of several lines, according to the convertion of four octahedral complexes of Mn^{2+} to the fifth octahedral complex Mn^{2+} (I).

Insert Figure 13

7. POLARIZED OPTICAL ABSORPTION MEASUREMENTS

Green Spodumene:- In figure 14 we see the optical absorption spectra of a greenish sample, obtained in three different orientations of polarized radiation. These spectra are similar to those observed in epidote (Burs and Strens, 1967), and so we assign to the same center: Mn^{3+} in distorted octahedral site. In octahedral site the Mn^{3+} ion have the fundamental electronic configuration $(t_{2g})^3(e_g)^1$ corresponding to a $5E_g$ state. The excited quintet state is $^5T_{2g}$. The spin allowed transition $^5E_g \rightarrow {^5T_{2g}}$ is of very low intensity.

Insert Figure 14

The $A\ell^{3+}$ spodumene site of octahedral coordination is compressed along the electronic z axis, and loose the center of symmetry. The e_g state splits to $^5A_1(d_{z^2})$ and $^5B_1(d_{x^2-y^2})$ configuration and the t_{2g} state splits to $^5E(d_{xz},d_{yz})$ and $^5B_2(d_{xy})$ configurations. The $^5A_1$ configuration is not occupied in the fundamental state. So, the electronic transitions will be:

$$^5B_1 \rightarrow {}^5A_1 : \; 10{,}500 \text{ cm}^{-1} \quad ,$$

$$^5E \rightarrow {}^5A_1 : \; 15{,}770 \text{ cm}^{-1} \quad ,$$

$$^5B_2 \rightarrow {}^5A_1 : \; 21{,}500 \text{ cm}^{-1} \quad .$$

The transitions a and b are more polarized in the plane perpendicular to the z axis. So, the 10,500 cm^{-1} band is assigned to the $^5B_1 \rightarrow {}^5A_1$ transition and the band 21,500 cm^{-1} to $^5B_2 \rightarrow {}^5A_1$. On the other hand, the absorption in 15,770 cm^{-1} is due to the $^5E \rightarrow {}^5A_1$ transition, being stronger with the polarized radiation in the plane containing the z axis. The separation energy Δ between the degenerate states e_g and t_{2g} is calculated as being 12,500 cm^{-1}, a value comparable to that found in epidote (13,450 cm^{-1}) and in viridine (13,100 cm^{-1}) in which Mn^{3+} in octahedral site is responsible for the color (Burns and Strens, 1967).

Lylac Spodumene:- The polarized optical absorption measurements in lylac spodumene are shown in figure 15. In this case the octahedral site occupied by Mn^{3+} is more compressed along the z axis than in green spodumene, increasing the values of the transition energies. The spectral bands of lylac spodumene were assigned to the following transitions:

$$^5B_1 \rightarrow {}^5A_1 : \; 12{,}000 \text{ cm}^{-1} \quad ,$$

$$^5E \rightarrow {}^5A_1 : \; 18{,}570 \text{ cm}^{-1} \quad ,$$

$$^5B_2 \rightarrow {}^5A_1 : \; 21{,}500 \text{ cm}^{-1} \quad ,$$

Insert Figure 15

The separation energy Δ is 13,400 cm^{-1}, comparable to those found in epidote and viridine. Also this value is bigger than that one found in green spodumene, accordingly to the shorter metal-oxygen bond in lylac spodumene.

8. DISCUSSION

In the previous sections of the present report we have shown several evidences that the absorption bands in kunzite are accounted by transition metal impurities diluted in its structure. Analysis of the concentrations of transition metals showed that the principal impurities are Mn and Fe. The EPR studies showed that Fe^{3+} remains practically constant after irradiation and heat treatments, showing that Fe^{3+} does not take place in the color change process. A very low intensity broad band at 12,000 cm^{-1}, assigned to Fe^{2+}, does not contribute to color in the samples. So, iron valence changes do not take part directly in color changes spodumene.

On the other hand, our experimental data show evidences that the optical absorption bands at room temperature are in fact associated to impurities: a) relative low doses of radiation form the bands which saturate at about 15 KGy, showing the total conversion of precursor defects; b) the saturation intensities are correlated to the Mn concentration.

The qualitative sketch of Claffy (1953) in which the colorless spodumene change to lylac must be revised. In the present report we show that in colorless samples, both green and lylac bands raise simultaneously, with the higher intensities bands at 15,770 and 29,400 cm^{-1} bands masking the 18,570 cm^{-1} band. Moderate heating (below 200°C) or moderate exposition to ultraviolet irradiation bleached at 15,770 cm^{-1} band and diminished the intensity of the 29,400 cm^{-1} band. The 18,570 cm^{-1} band appears and the spodumene turns lylac. This band and the remaining part of the 29,400 cm^{-1} band are annealed on heating at higher temperatures (400°C) or long exposition to ultraviolet light and the sample turns colorless. The X-Rays or γ-Rays irradiation turns the lylac sample green. Finally, X-Rays and γ-Rays irradiation of colorless samples obtained by heating or ultraviolet exposition, raises all bleached bands, giving a cyclic character to the process. This is sketched in figure 16.

Insert Figure 16

Let us analyse the optical absorption bands in function of possible valence changes of Mn substitutional to $A\ell^{+3}$. The Schmitz and Lehmann's model where green and lylac bands arise from valence changes of Si substitutional Mn^{2+} in Mn^{3+} and Mn^{4+}, respectively, seems questionable by two reasons: a) the EPR spectra do not show evidences for Si substitutional Mn^{2+}; b) 15,770 and 18,570 cm^{-1} bands raise independently, showing that they do not arise from valence interconversion in the same impurity.

In the elaboration of a model for color changes in spodumene, we must consider that while the 15,770 and 18,570 cm^{-1} bands are completely annealed on heating at 400°C, the Mn^{2+} EPR spectra of preheated samples do not show any changes on heating and irradiation. So, Mn^{2+} is not associated to color changes. This is reinforced by the observation that the EPR spectra do not change in samples bleached by UV irradiation.

We examined the possibility that the green and lylac bands were due to Mn^{4+} in octahedral field as found in $Li_2(Ti,Mn)O_3$ (Lorenz and Prener, 1956). Here the 14,800 cm^{-1} band was assigned to the ${}^4A_2(t_3) \rightarrow {}^2E(t_3)$ transition. This possibility was deleted because in powder EPR spectra Mn^{4+} lines were not observed.

On the other hand, our polarized optical absorption measurements were explained as being due to Mn^{3+} in distorted octahedral sites. The site in spodumene showing such type of distortion is due to substitution of $A\ell^{3+}$. Assuming that the Mn, present as impurity in spodumene, is stabilized as Mn^{3+} in $A\ell^{3+}$ site, we suggest the following explanation for the present observations.

In colorless samples Mn^{3+} absorption bands are not observed due to their low intensity. The transition probability is proportional to the integral:

$$P \ \alpha \int \psi_F \ \mu_z \ \psi_E \ dz \quad ,$$

where μ_z is the dipole moment component along z, ψ_F and ψ_E are the wave functions of the Mn^{3+} in fundamental and excited states. As the wave functions of d orbitals are symmetric, P=0 for octahedral symmetry. There are two cases were P does not vanishes:

a) Distortion of the Octahedra. The $A\ell^{3+}$ site in spodumene is distorted (Deer et al, 1966) as shown in figure 17. If this distortion is not modified by substitution with Mn^{3+} , the forbidden d-d transition is removed, because the mixture of 3d and 4p orbitals occur in some extent. The wave functions of Mn^{3+} are changed to

Insert Figure 17

$$\psi_F = a_F\psi_F^d + b_F\psi_F^s \quad , \quad \psi_E = a_E\psi_E^d + b_E\psi_E^s \quad ,$$

where ψ^d is d orbital and ψ^s is the wave function giving the 4s orbital mixture, a and b are adimensional coefficients. In this case:

$$P_{cc} \; \alpha \int \psi_F^s \, \mu_z \, \psi_E^d \, dz + \int \psi_F{}^d \mu_z \, \psi_E^s \, dz \quad .$$

The magnitude of $\underline{P}$ depends on the degree of mixture of the orbitals 3d and 4s.

b) Covalent Character of Mn - O Bond. Net atomic changes for each atom in spodumene were estimated by the X-Ray method (Sasaki et al, 1980) giving $A\ell = +2.4$, $Li = +0.7$, $Si = +2.4$ and $0 \cong -1.3$. This shows that the Si-O bond is strongly covalent, and that the $A\ell^{3+}$ bond with the surrounding oxygens show covalent character on some small extent. Due to the covalent character the wave function of Mn^{3+} is modified to:

$$\psi_F = c_F \, \psi_F^{cc} + d_F \, \psi_F^e \quad , \quad \psi_E = c_E \, \psi_E^{cc} + d_E \, \psi_E^e$$

where ψ^{cc} is the wave function of Mn^{3+} in a distorted octahedral crystal field and ψ^e is the wave function of the oxygen, a and b are adimensional coefficients. In this case:

$$\underline{P} \; \alpha \; \underline{P}_{cc} + \int \psi_F^{cc} \, \mu_z \, \psi_E^e \, dz + \int \psi_F^e \, \mu_z \, \psi_E{}^{cc} dz \quad .$$

The symmetry of the absorption spectra is now dependent of the symmetry of the wave functions of the oxygens.

In manganiferrous epidote piemontite (Burns and Strens, 1967) it was observed the Mn^{3+} absorption spectrum in a distorted octahedral site. In this sample the concentration is high, being about 10^4 ppm. This suggests that $\underline{P}$ is small and the mixture of orbitals, 3d-4p due to distortion and the covalent character of Mn-O bond are not enough to remove completely the d-d forbidden transition character. In this way, the Mn^{3+} in similar distorted octahedral site of other crystals is expected to give measurable absorption only for high concentrations. This is consistent with the observation that our samples, which show small concentrations of Mn , became colorless by thermal and/or optical bleaching.

The irradiation induced optical absorption assigned to Mn^{3+} is probably produced by the trapping of electrons or holes. The substitution of $A\ell^{3+}$ by Mn^{3+} alters the charge distribution around the group MnO_6 . The charge unbalance between the groups $A\ell O_6$ and MnO_6 turns the later an electron trap. The raising of the intensity of the d-d transition by charge trapping can occur through the increasing of the covalent character in Mn-O bond. As the polarized spectrum shows a maximum in z direction, we suggest that the electron is capturated in one of the two oxygens in the z-axis. This electron occupies the 4s orbital of the z-axis oxygen allowing a good coupling for the oxygen wave function with d_{z^2}, d_{xz} and d_{yz} Mn orbitals explaining thus the higher absorption intensity of the $^5E \rightarrow {}^5A_1$ (18,170 cm^{-1}) band and the weak $^5B_1 \rightarrow {}^5A_1$ (12,000 cm^{-1}) and $^5B_1 \rightarrow {}^5A_1$ (22,000 cm^{-1}) bands.

Considering the Mn^{3+} in octahedral site with tetragonal distortion, we obtained from the polarized spectra the values for the parameter Dq (octahedral field), Ds and Dt (tetragonanal distortion) given in table 5, for green and lylac bands. In both cases we got $B \cong 800$ cm^{-1} .

Insert Table 4

Our results about thermal decay kinetics of the optical absorption bands of spodumene remains without a conclusive interpretation. We verified that the simple models usually applied for electron and hole kinetics cannot be used in spodumene. Even some more elaborated models, like coupled kinetics model, failed to explain the observed behavior. The numerical fit obtained with three exponentials suggest that the kinetics is composed by three 1st order processes keeping their own identity on the temporal point of view: one of the processes predominates in the initial time of the annealing; the second one at higher annealing times and a third one at longer times. The main difficulty of this interpretation was the observation that the pre-exponential factors (giving the relative initial concentrations of the species which recombine with the center responsible for the optical absorption band) showed great variations with temperature. We suggest that more detailed studies should be done. Here we take only the hypothesis that the increase of temperature favours diffusion processes of such species and contributes to the changes from low, intermediate and fast processes. In any way, we determined the activation energies for the decay of different species, obtaining values of decimal order of electron-volt, the same as found in processes involving impurities in minerals. On the other hand, the values for the mean life at room temperature obtained for the green and lylac center are coherent with the observations by gemologists, so that the lylac center is stable in dark, and the green center is unstable.

ACKNOWLEDGMENTS

We would like to thank Prof. Shigueo Watanabe (IFUSP), Prof. Antonio R.P.L. Albuquerque (FEI) and Prof. Walter M. Pontuschka for the support and discussions which enriched this work. Our thanks to Prof. Osvaldo Luis Dias (DF UFGo) for the X-ray fluorescence measurements, and to EMBRARAD SA. for the use of their 60 γ-rays source.

This work was supported by grants of CNPq and FINEP.

REFERENCES

1) Anderson, P.W. and Weiss, P.R. (1953), Exchange Narrowing in Paramagnetic Resonance, Rev. Mod. Phys. 25, 269-276.

2) Bevington, P.R. (1969), Data Reduction and Error Analysis for the Physical Sciences, McGraw-Hill Book Comp., N.York, p.204.

3) Burns, R.G. and Strens, R.G.J. (1967), Structural Interpretation of Polarized Absorption Spectra of the $A\ell$-Fe-Mn-Cr Epidotes, Miner. Magaz. 36, 204-225.

4) Claffy, E.W. (1953), Composition, Tenebrescence and Luminescence of Spodumene Minerals, Amer. Miner. 38, 919-923.

5) Deer, W.A., Howie, R.A. and Zussman, J. (1966), Rock Forming Minerals, vol. 2, Longman, London, p.92.

6) Dexter, D.L. (1954), Shapes of Absorption and Emission Lines of Impurities in Solids, Phys. Rev. 96, 615-616.

7) Fuller, G.E. and Moran, P.R. (1976), USAEC Technical Report COD-1105, p.203.

8) Hassan, F. and Labib, M. (1978), Induced Color Centers in α-Spodumene Called Kunzite, Neues Jb. Miner. Abh. 134, 104-115.

9) Holuj, F. (1968), EPR of Mn^{++} in Spodumene. I. Natural Crystals, Canad. J. Phys. 46, 287-301.

10) Isotani, S., Toledo, D.H., Ito, A.S. and Pontuschka, W.M. (1982), Um Método de Ajuste da Função $n(t)=n_o(1+at)^b$, Semina 3, 123-125.

11) Levy, P.W., Mattern, P.L., Lengweiler, K. and Bishay, A.M. (1974), Studies of Nonmetals During Irradiation: V, Growth and Decay of Color Centers in Barium Aluminoborate Glasses Containing Cerium, J. Am. Ceram. Soc. 57, 176-181.

12) Lorenz, M.R. and Prener, J.S. (1956), Effect of Crystal Structure Upon the Luminescence of Manganese-Activated Lithium Titanate, J. Chem. Phys. 25, 1013.

13) Lushchick, C.B. (1956), The Investigation of Trapping Centers in Crystals by the Method of Thermal Bleaching, Sov. Phys. JETP 3, 390-399.

14) Maxia, V., Onnis, S. and Rucci, A. (1971), On the Analysis of Thermoluminescence Kinetics, J. Lumin. 3, 378-388.

15) Randall, J.F. and Wilkins, M.H.F. (1940), Phosphorescence and Electron Traps. I. The Study of Trap Distributions, Proc. Royal Soc. A184, 366-389.

16) Sasaki, S., Fujino, K., Takeuchi, Y. and Sadanaga, R. (1980), On the Estimation of Atomic Charges by the X-Ray Method for some Oxides and Silicates, Acta Cryst. A36, 904-915.

17) Schmitz, B. and Lehmann, G. (1976), Color Centers of Manganese in Natural Spodumene $LiA\ell Si_2O_6$, Ber. Buns. Phys. Chem. 79, 1044-1049.

18) Takeuchi, N., Inabe, K. and Nanto, H. (1975), Note on the Isothermal Decay Method for Determining Trap Depth from Glow Curves, 10, 159.

TABLE 1 - Impurity concentrations of Cr, Fe and Mn in spodumene

Sample	Color	Cr	Fe	Mn	Mn/Fe
1	lylac	80 ± 20	135 ± 8	240 ± 10	1.78
2	lylac	80 ± 20	102 ± 7	390 ± 10	3.82
3	lylac	90 ± 20	165 ± 8	460 ± 10	2.79
4	colorless	90 ± 20	472 ± 8	290 ± 10	0.61
5	colorless	60 ± 20	327 ± 7	240 ± 10	0.73

TABLE 2 - Parameter of optical absorption bands line shape fit

ν_{oi} (cm^{-1})	σ_i ($10^3\ cm^{-1}$)	y_{oi} (cm^{-1})		
		green	lylac	colorless
15.77 ± 0.06	1.2 ± 0.1	1.65	0.10	-
18.57 ± 0,02	1.08 ± 0.08	0.69	0.69	-
29.4 ± 0.4	2.7 ± 0.1	10.30	8.60	-

TABLE 3 - Parameters of thermal decay kinetics fit for three exponentials model

T(°C)	a_1	b_1	a_2	b_2	a_3	b_3
128	0.86 ± 0.04	0.00052 ± 0.00027	0.12 ± 0.03	0.025 ± 0.013	0.022 ± 0.016	0.085 ± 0.054
138	0.64 ± 0.04	0.00069 ± 0.00023	0.26 ± 0.03	0.017 ± 0.003	0.096 ± 0.018	0.14 ± 0.04
156	0.44 ± 0.03	0.00150 ± 0.00040	0.36 ± 0.02	0.028 ± 0.004	0.190 ± 0.025	0.20 ± 0.03
178	0.290 ± 0.007	0.0024 ± 0.0002	0.32 ± 0.01	0.048 ± 0.003	0.380 ± 0.017	0.35 ± 0.02
197	0.150 ± 0.002	0.0046 ± 0.0001	0.26 ± 0.08	0.079 ± 0.003	0.59 ± 0.01	0.71 ± 0.03
210	0.100 ± 0.002	0.0061 ± 0.0002	0.18 ± 0.01	0.099 ± 0.004	0.72 ± 0.01	0.99 ± 0.04
303	0.900 ± 0.008	0.00098 ± 0.00006	0.073 ± 0.024	0.024 ± 0.013	0.024 ± 0.024	0.10 ± 0.09
334	0.59 ± 0.04	0.0022 ± 0.0003	0.34 ± 0.03	0.031 ± 0.005	0.07 ± 0.02	2.1 ± 0.1
356	0.37 ± 0.01	0.0046 ± 0.0002	0.37 ± 0.02	0.041 ± 0.004	0.26 ± 0.02	0.26 ± 0.03
371	0.31 ± 0.01	0.0066 ± 0.0002	0.350 ± 0.008	0.046 ± 0.003	0.34 ± 0.01	0.46 ± 0.03
383	0.090 ± 0.004	0.0086 ± 0.0004	0.430 ± 0.006	0.073 ± 0.002	0.48 ± 0.01	0.96 ± 0.08

TABLE 4 - Crystal field parameters of green and lylac

bands	Dq (cm^{-1})	D_s (cm^{-1})	D_t (cm^{-1})
green	1.100	-2.300	-250
lylac	1.200	-2.350	-500

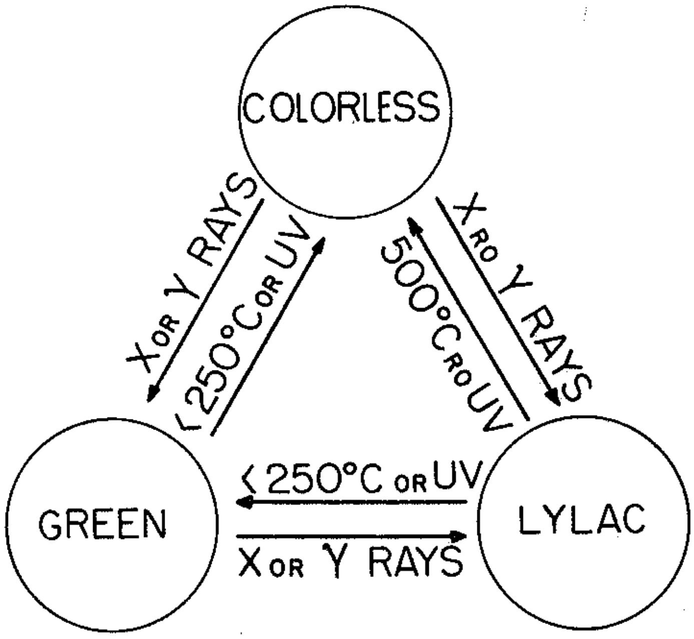

Figure 1 - Sketch of the process of transformation of colour of spodumene by heating and irradiations as proposed by Claffy.

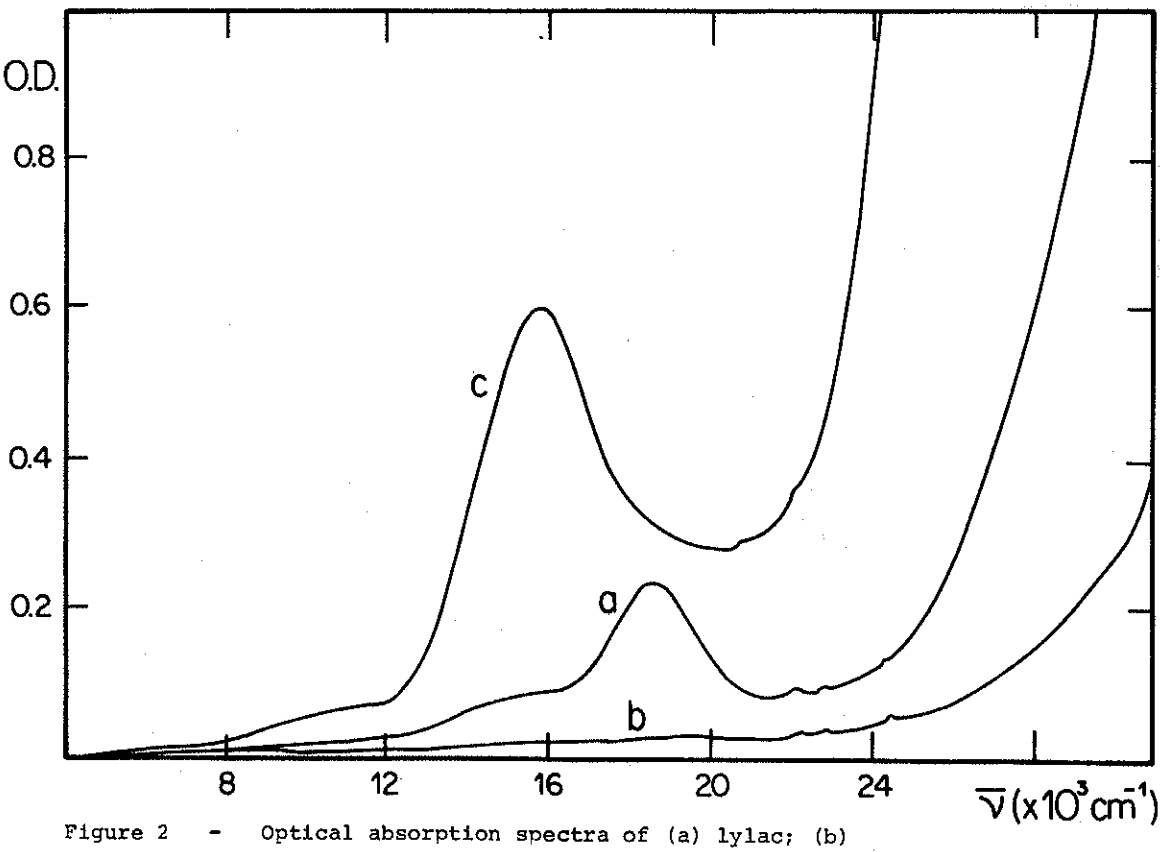

Figure 2 - Optical absorption spectra of (a) lylac; (b) colorless and (c) ^{60}Co γ-rays irradiated samples of spodumene.

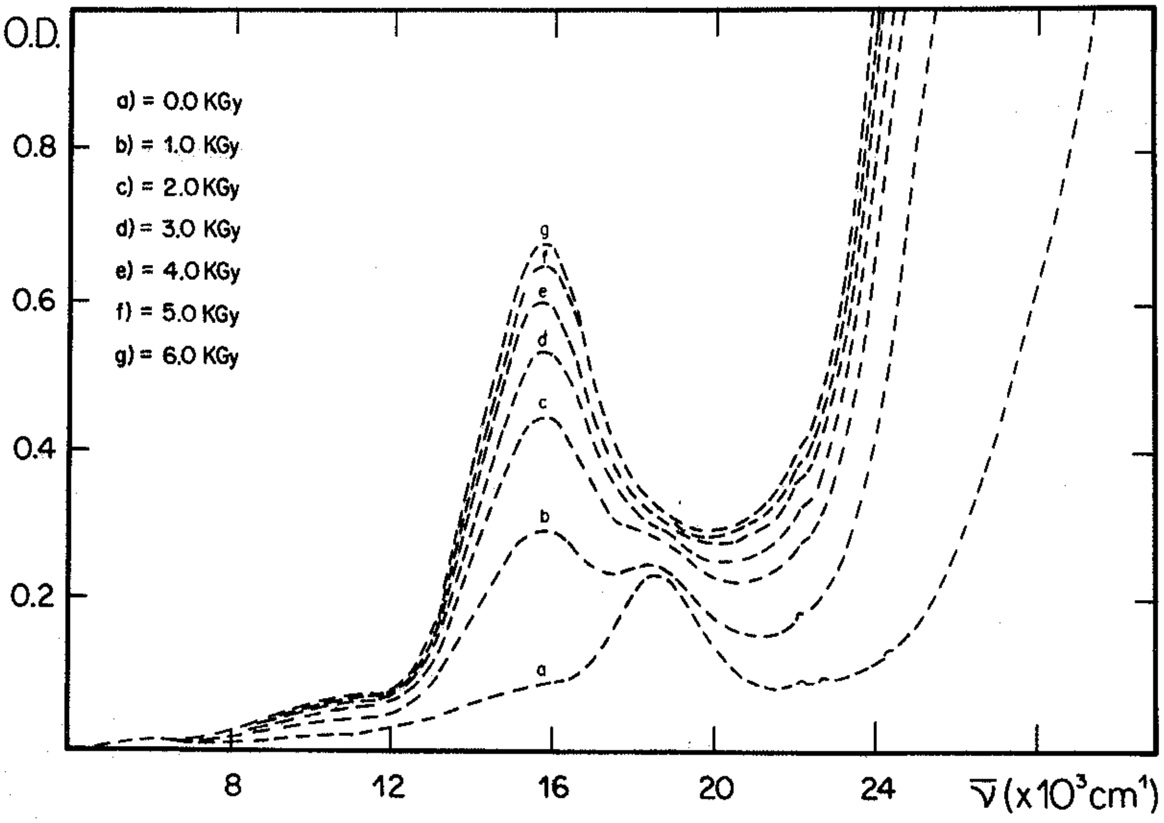

Figure 3 - Optical absorption spectra of ^{60}Co γ-rays irradiated spodumene.

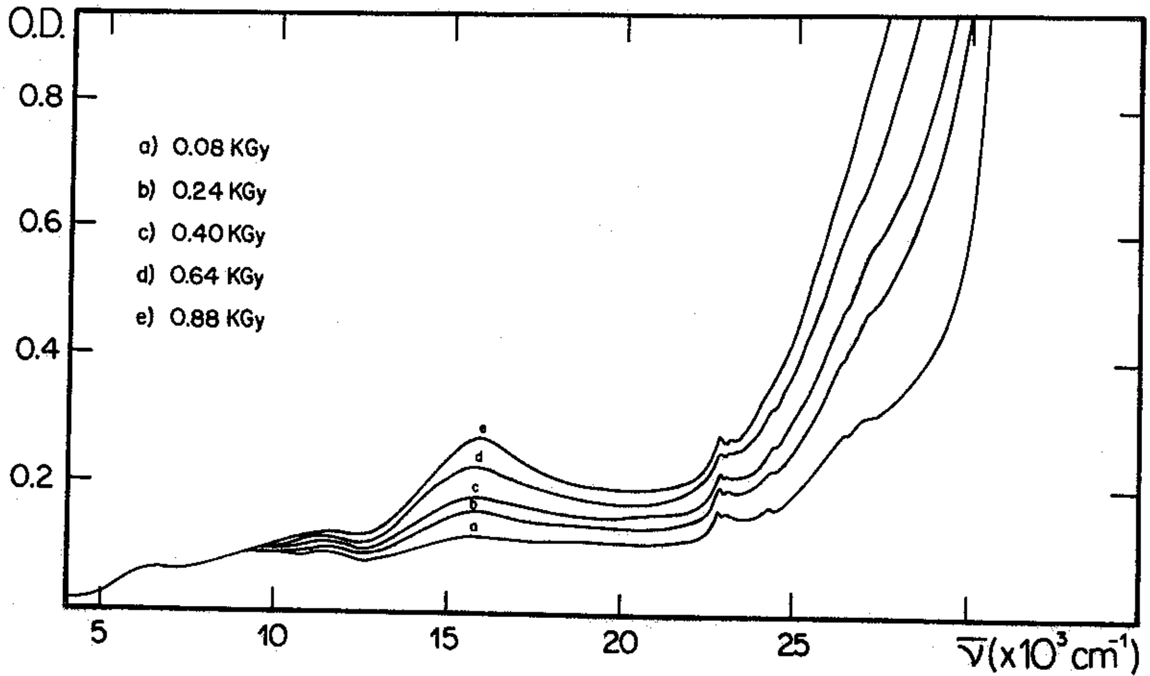

Figure 4 - Optical absorption spectra of ^{60}Co γ-rays irradiated colorless spodumene.

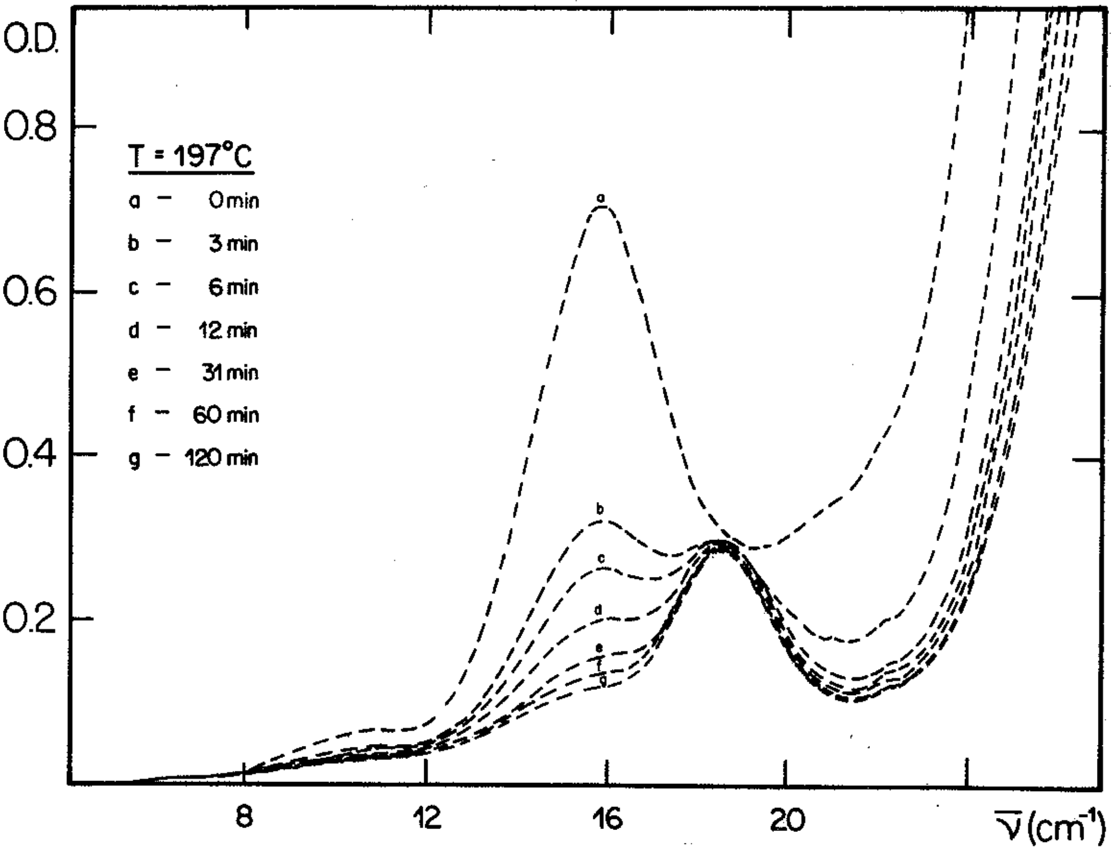

Figure 5 - Optical absorption spectra of ^{60}Co γ-rays irradiated lylac spodumene heated at 197°C.

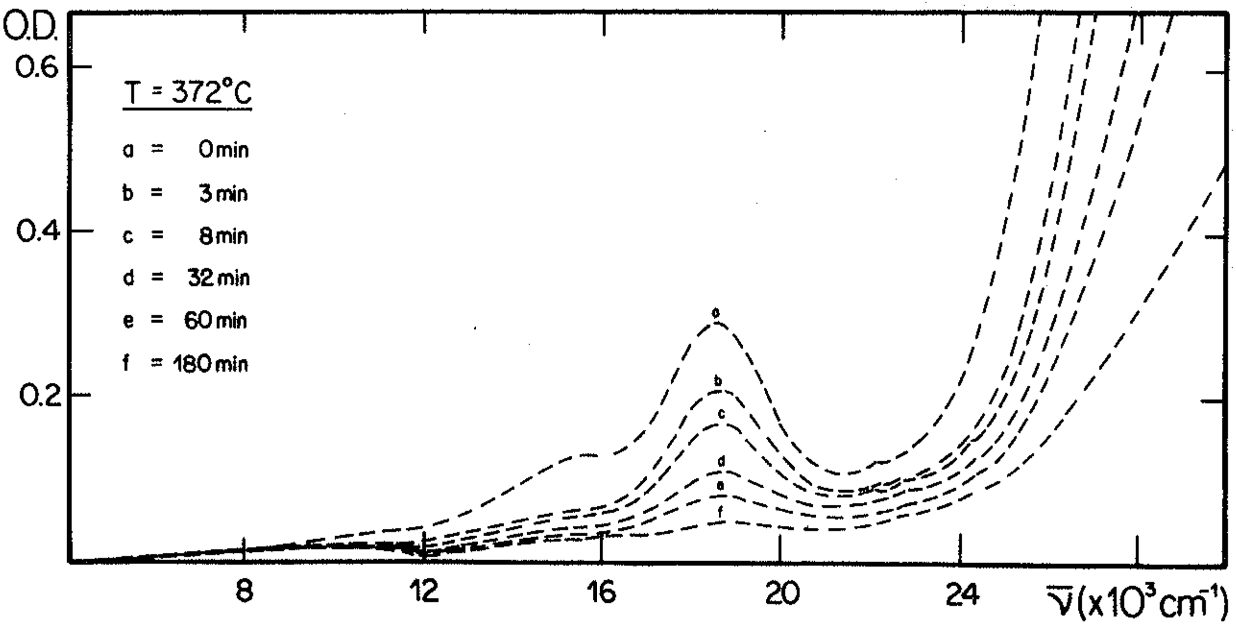

Figure 6 - Optical absorption spectra of lylac spodumene heated at 372°C.

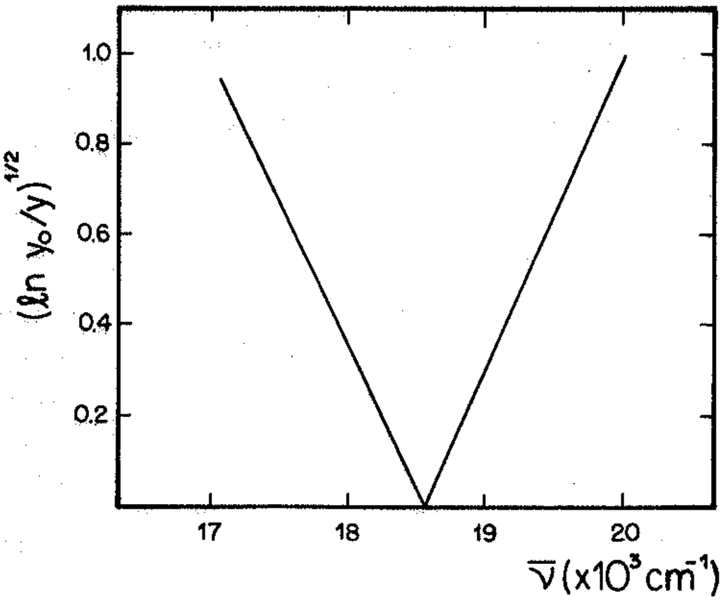

Figure 7 - Correlation between $|\,\ell n(y_o/y)\,|^{1/2}$ as function of ν (cm^{-1}). Here y is the absorption intensity, y_o the maximum absorption and ν is the wavenumber.

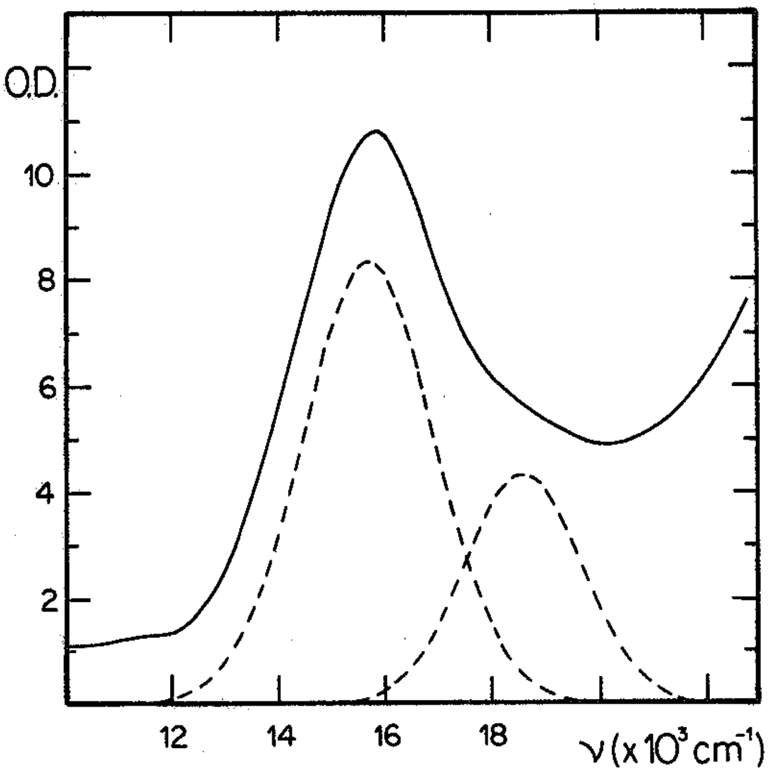

Figure 8 - Fit of spectrum of ^{60}Co γ-rays irradiated lylac spodumene.

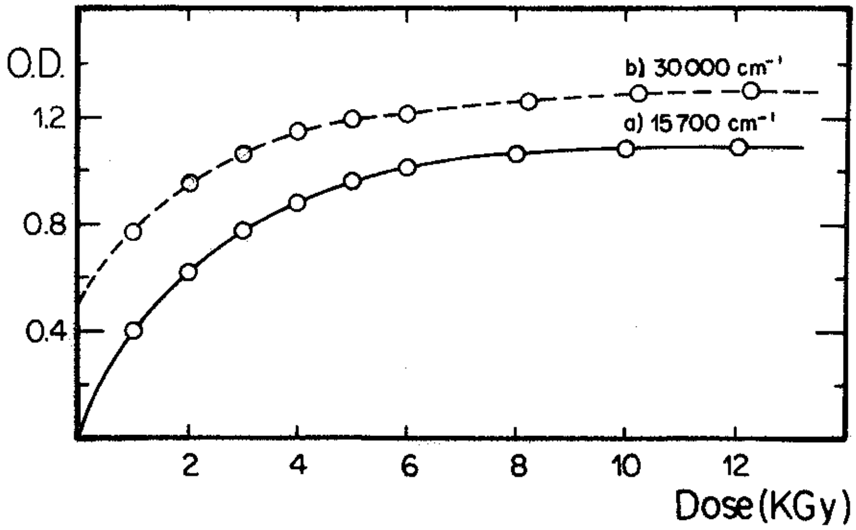

Figure 9 - Growth of (a) 15,700 cm^{-1} and (b) 30,000 cm^{-1} bands with irradiation dose.

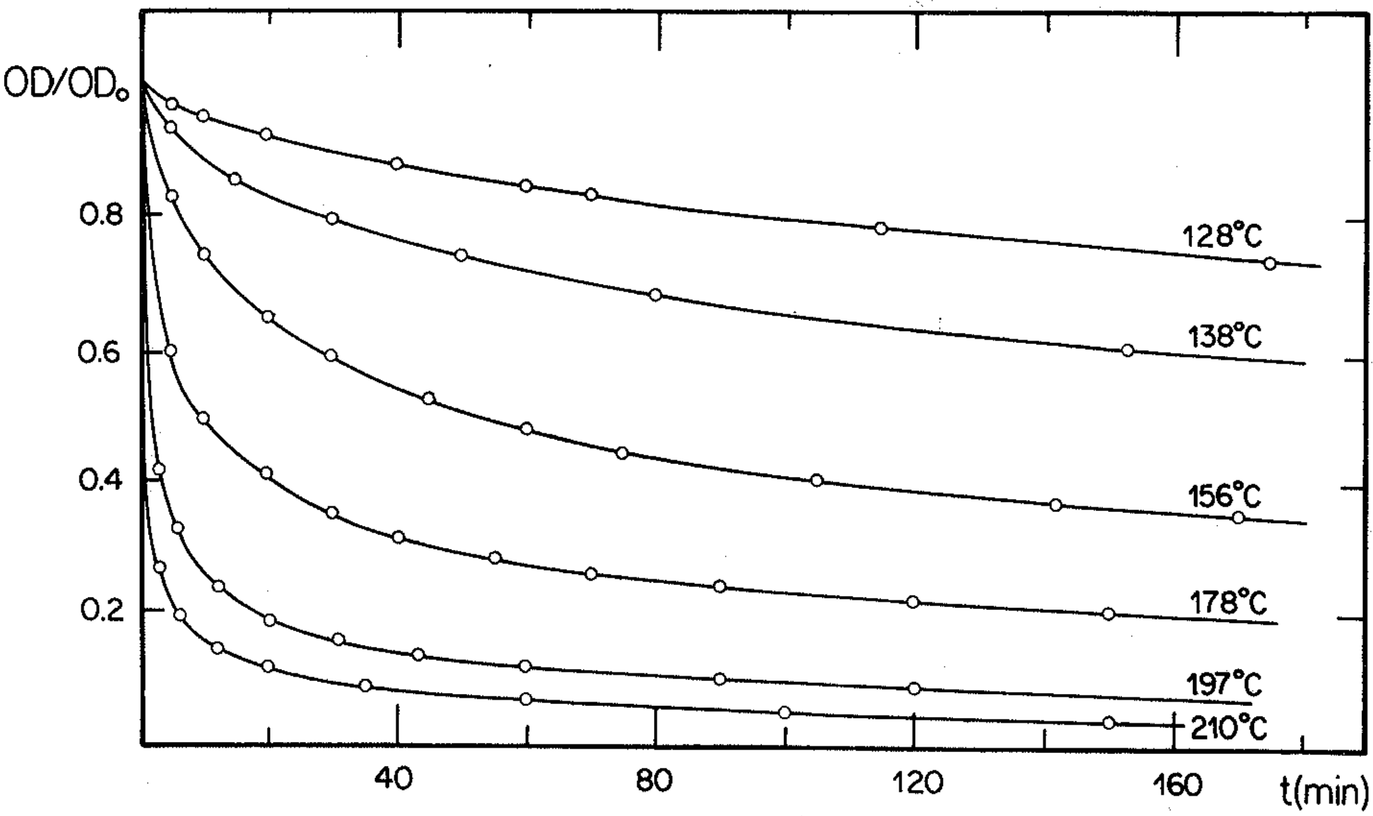

Figure 10 - Kinetics of the band at 15,700 cm^{-1}.

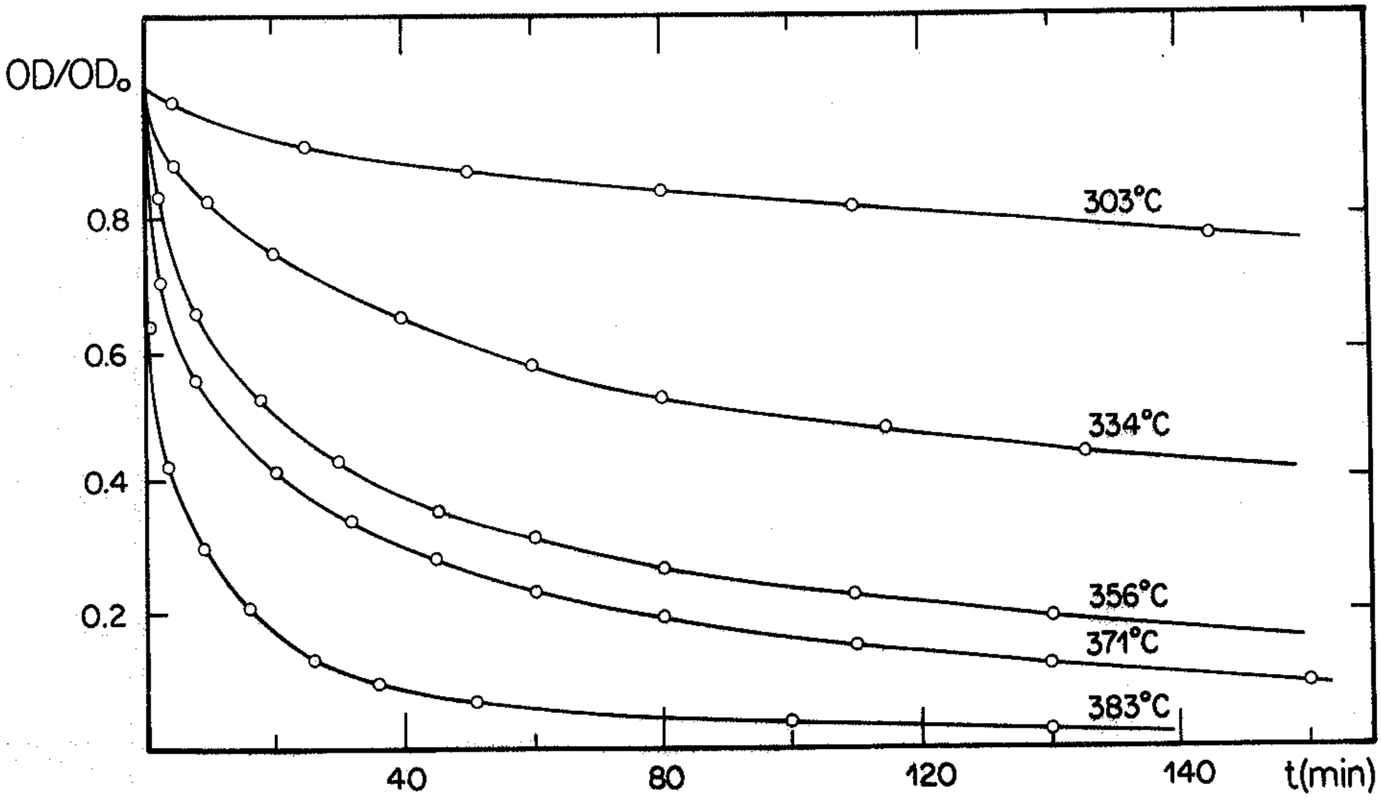

Figure 11 - Kinetics of the band at 18,570 cm^{-1}.

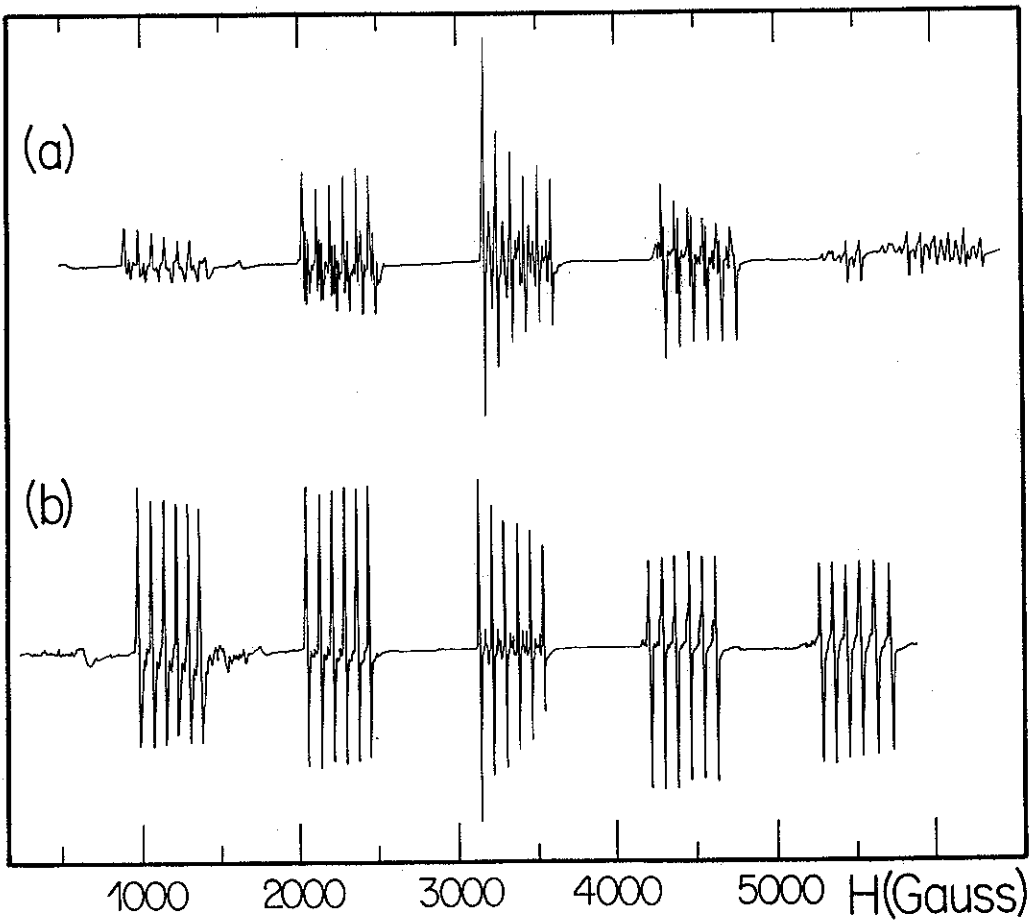

Figure 12 - EPR spectra of H // z lylac spodumene.

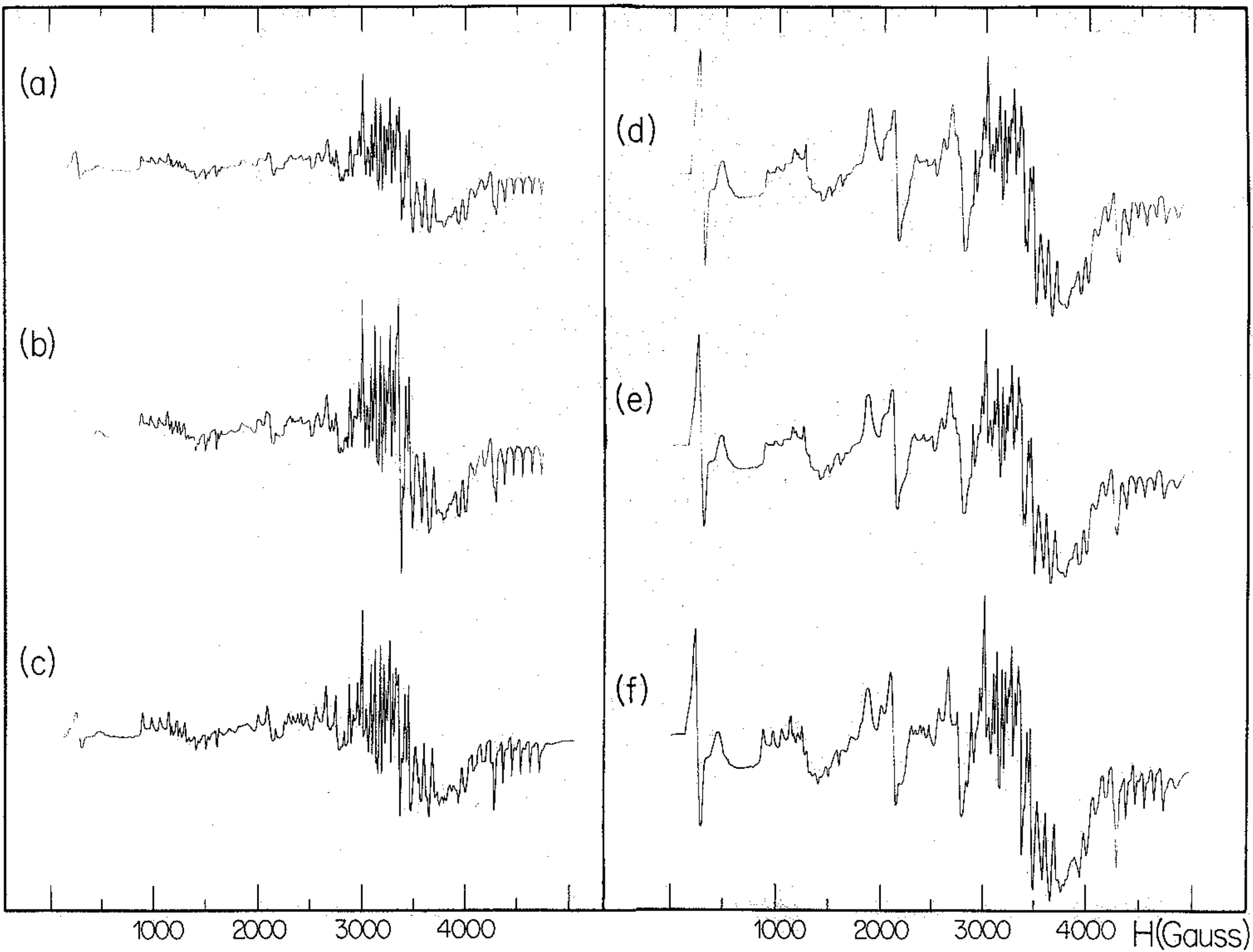

Figure 13 - EPR spectra of powder lylac spodumene.

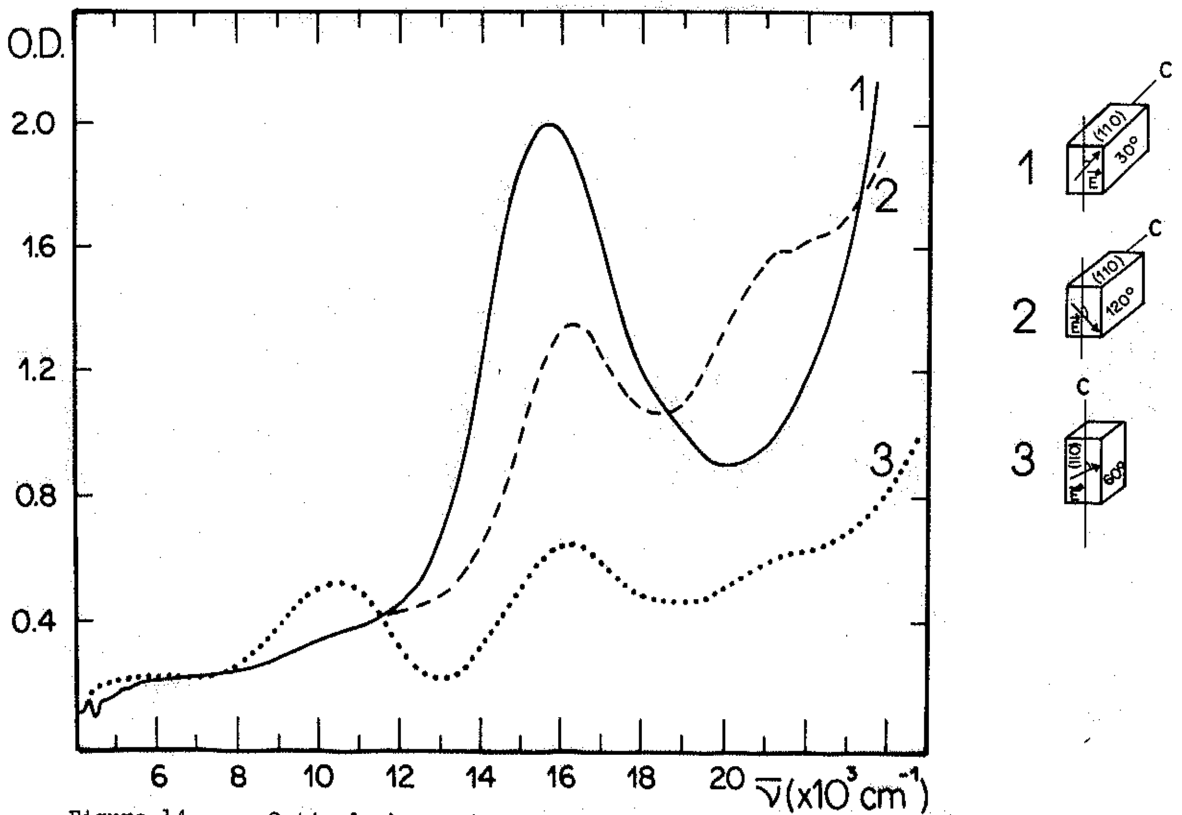

Figure 14 - Optical absorption spectra of irradiated spodumene in three different orientations.

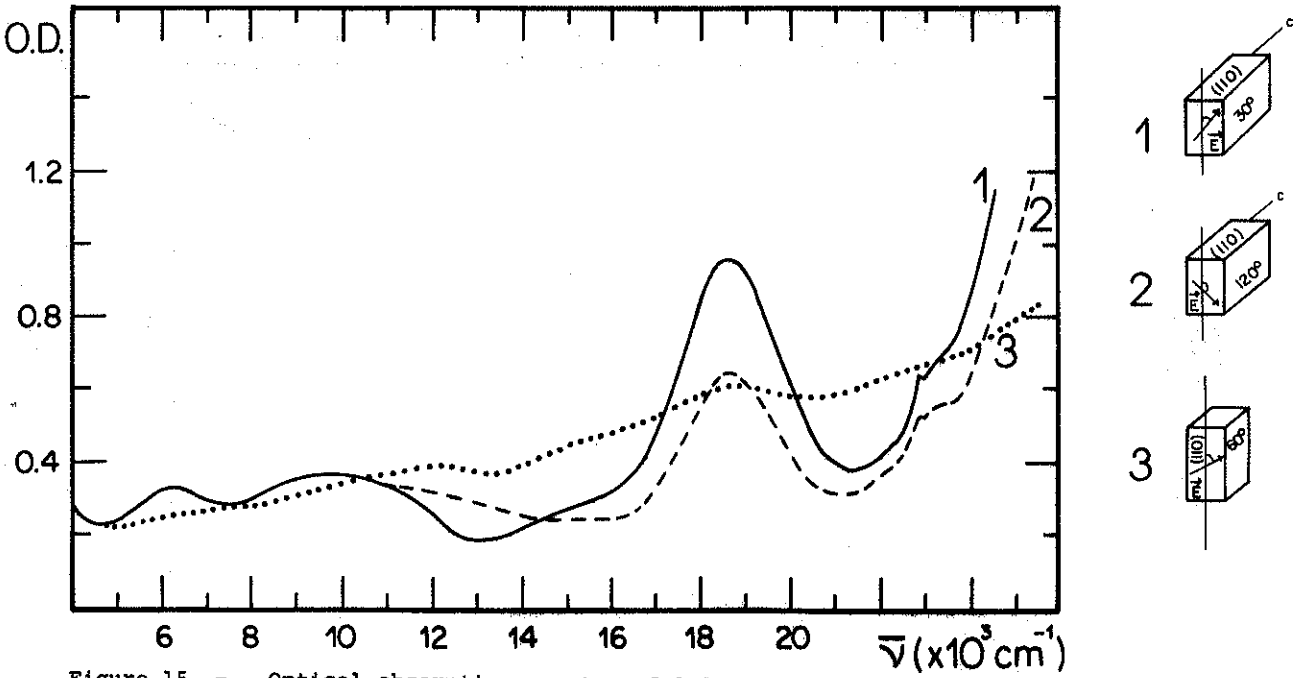

Figure 15 - Optical absorption spectra of lylac spodumene in three different orientations.

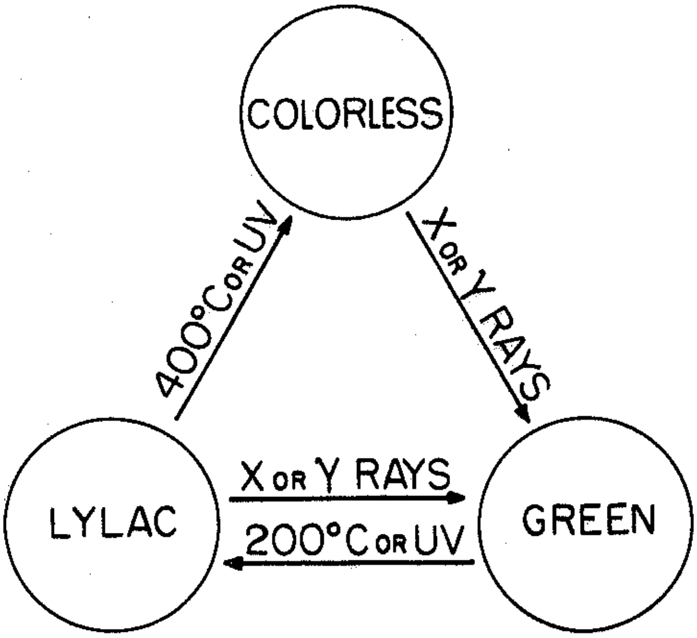

Figure 16 - Sketch of the process of transformation of colour of lylac and colorless spodumene by heating and irradiations as shown in the present report.

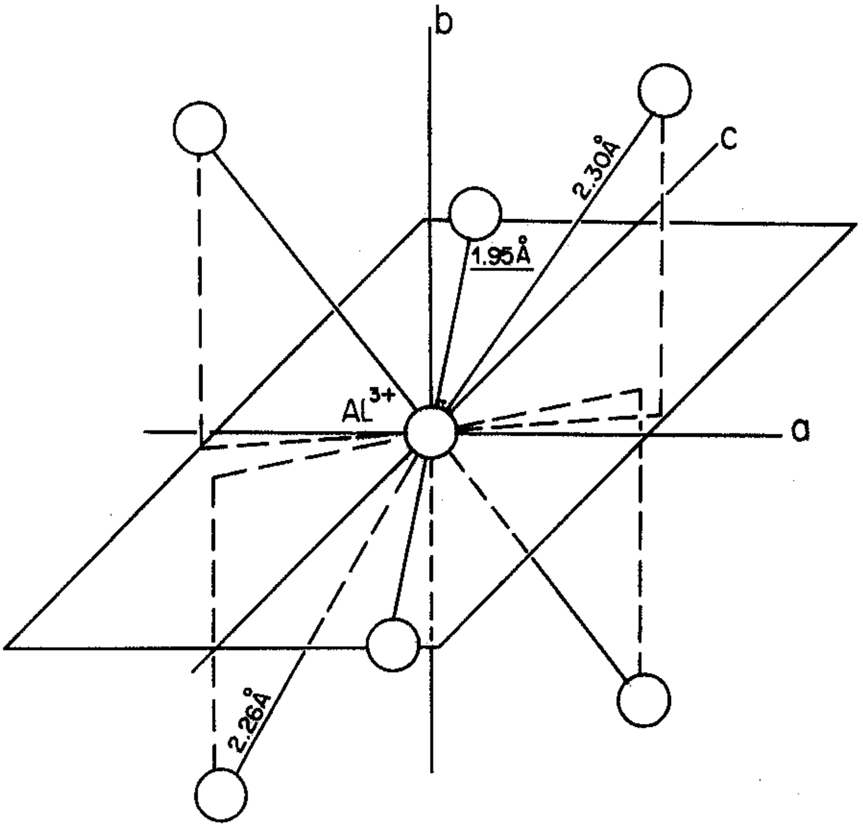

Figure 17 - Sketch of the oxygen ions around Al^{3+} ions.